Effect of pulsed laser action on hole-energy spectrum of Ge/Si self-assembled quantum dots

A. I. Yakimov,* A. V. Dvurechenskii, V. A. Volodin, M. D. Efremov, A. I. Nikiforov, and G. Yu. Mikhalyov
Institute of Semiconductor Physics, Siberian Branch of the Russian Academy of Sciences, Prospekt Lavrent'eva 13, 630090 Novosibirsk, Russia

E. I. Gatskevich and G. D. Ivlev
Institute of Electronics, National Academy of Sciences of Belarus, 22 Logoiskii Trakt, 220090 Minsk, Belarus
(Received 25 April 2005; published 16 September 2005)

Space-charge spectroscopy has been used to study the hole energy spectrum of an array of Ge quantum dots (QD's) coherently embedded in a Si matrix and subjected to a ruby laser ($\lambda = 694$ nm) nanosecond irradiation *ex situ*. The laser energy density in a single pulse was near the melting threshold of the Si surface. The number of laser pulses was varied from 1 to 10, and the duration of each pulse was 80 ns. From the capacitance-voltage characteristics, temperature- and frequency-dependent admittance measurements, the energies of holes confined in Ge QD's were determined. The pulsed laser annealing was found to result in a deepening of the hole energy level relative to the bulk Si valence band edge and in a decrease of the hole energy dispersion. After the treatment with ten laser pulses, the spread of the hole energies due to varying sizes of the QD's within the ensemble was reduced by a factor of about 2. The obtained results give evidence for a substantial reduction of the QD's size dispersion and for a narrowing distribution of the hole energy levels stimulated by nanosecond laser irradiation. A possible explanation of the improved uniformity of QD's sizes involves dissolving small size Ge QD's in a Si matrix by pulsed laser melting of the Ge nanoclusters and their subsequent intermixing with surrounding solid Si.

DOI: 10.1103/PhysRevB.72.115318 PACS number(s): 73.21.La, 73.40.Gk, 73.63.Kv

I. INTRODUCTION

An elegant way to fabricate large-scale arrays of zero-dimensional semiconductor structures (quantum dots, QD's) is based on strain-induced self-assembly of islands during heteroepitaxial growth of lattice mismatched semiconductors. Ideal QD's exhibit atomiclike properties due to their three-dimensional carrier confinement. The discrete energy spectrum of QD's renders them extremely promising for the development of semiconductor lasers,[1] photodetectors,[2] single-electron,[3] and single-photon devices,[4] as well as quantum computation.[5] A narrow distribution of energy levels of carriers confined within an ensemble of self-organized QD's and a large energy separation between the quantized states ($> k_B T$, k_B is the Boltzmann constant and T is the temperature) are the crucial issues when QD's are considered for both device applications and fundamental physical studies. But this still remains a challenging subject. To obtain atomiclike density of electronic states (DOS), it is necessary to reduce geometrical size of the dots, that can be achieved by decreasing the growth temperature.[6] However, QD's fabricated at low temperatures are characterized by large (up to 50%) dispersion of the dot size.[7] In turn, statistical fluctuations of the QD size is a main source of inhomogeneous broadening of the DOS. For Ge/Si(001) QD's, several approaches have been exploited to tune the uniformity of the Ge island sizes and shapes, such as manipulating the substrate temperature[8,9] and the deposition sequence,[10] vertical ordering in QD multilayers,[11–13] surfactant-mediated growth,[14,15] deposition on vicinal,[16] and oxidized[17] surfaces, ion-beam stimulated growth.[18]

Despite some technological progress any information on how these approaches affect the energy spectrum of carriers confined in an ensemble of QD's is still missing. In this work we suggest an alternative way to improve the homogeneity of Ge/Si QD's sizes and present the unambiguous evidence that this approach certainly allows to reduce dispersion of hole energy levels in the dots. The idea was to dissolve Ge nanoclusters with the smallest size in the Si matrix by nanosecond pulsed laser melting of Ge dots and their subsequent intermixing with surrounding solid Si. The melting point of Ge (958.5 °C) is much less than that of Si (1410 °C). The short-pulse heating allows us to melt Ge nanoclusters while the Si matrix is kept solid. Ge solidification time is approximately the same for all molten Ge nanoclusters being defined by cooling of the Si environment due to the heat diffusion into the Si substrate. This time is comparable with the laser pulse duration.[19] Due to large interface/volume ratio, the smallest Ge QD's may be easily dissolved and hence disappear. As a result, only nanoclusters of larger size will survive giving rise to a more narrow size distribution in an ensemble of the dots.

II. EXPERIMENTAL PROCEDURES

Samples were grown by molecular-beam epitaxy on a p^+-Si(001) substrate with a resistivity of 0.005 Ω cm doped with boron up to a concentration of $\sim 10^{19}$ cm^{-3}. A Ge layer 6 monolayer thick (~8.5 Å) was introduced into the 0.7-μm epitaxial p-Si layer (boron concentration $\sim 3 \times 10^{16}$ cm^{-3}) at a distance of 0.4 μm from the substrate. The growth temperatures were 500 and 700 °C for the cap and buffer Si layers, respectively, but, during the growth of Ge, the temperature was lowered to 300 °C to fabricate small self-assembled Ge nanoclusters. From transmission electron

 ©2005 The American Physical Society

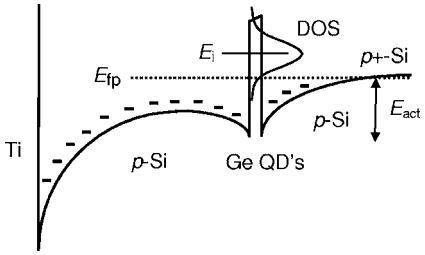

FIG. 1. The valence band profile of a Si Schottky diode with a layer of Ge quantum dots.

micrographs, we observe the Ge dots to be approximately 8–10 nm in diameter and 1 nm in height. The areal density of the dots is $n_{QD} \simeq 4 \times 10^{11}$ cm^{-3}. The reflection high-energy electron diffraction patterns of the surface of Ge film showed that the Ge nanoclusters have a pyramid shape. To separate response from the dots, the reference sample was grown under conditions similar to the dot sample, except that no Ge was deposited.

As the radiation source, we used a ruby laser with a wavelength of $\lambda = 694$ nm. The laser pulse was a nearly Gaussian temporal shape with a full width at half maximum being 80 ns. The spatial variation in the density of laser energy did not exceed ±5% over the laser spot of 4.5 mm in diameter. The energy density in a single pulse was close to 1 J cm^{-2}. For this value, the peak temperature of the heated Si surface reaches the Si melting point (1410 °C), whereas the temperature at the position of Ge nanoclusters is lower[20] (≈1200 °C), but still larger than the melting temperature of bulk Ge (958.5 °C). To control the temperature of the Si surface, a pyrometer sensor detected thermal radiation from the central part of the laser-heated area of the samples was used.[21] The samples were subjected to one or ten laser pulses.

The Raman spectra were measured at room temperature using a computer-controlled setup based on a DFS-52 spectrometer (LOMO, St. Petersburg); an Ar^+ laser ($\lambda = 514.5$ nm) was used as the pump for the Raman process. We used quasibackscattering geometry, the incident radiation was polarized along the <100> crystallographic direction, and the scattered light was detected in ⟨the <010>⟩ polarization. The chosen configuration is allowed for the scattering by longitudinal optical phonons in Ge and Si and forbidden for the two-phonon scattering by transverse acoustical phonons in the Si substrate. This enabled us to avoid confusions encountered when interpreting Raman spectra in Ge/Si heterostructures.[22]

For the capacitance and conductance measurements, Ti contacts were deposited on top of the samples through a shadow mask to form a Schottky diode. The area of the Ti contacts was $S \simeq (3.2-4.0) \times 10^{-3}$ cm^2. Figure 1 schematically displays the valence band of the QD sample at zero bias. The admittance was measured using a Fluke PM6306 meter in the frequency range $f = 10-700$ kHz at temperatures from 100 to 300 K. The amplitude of the ac modulation voltage was 25 mV.

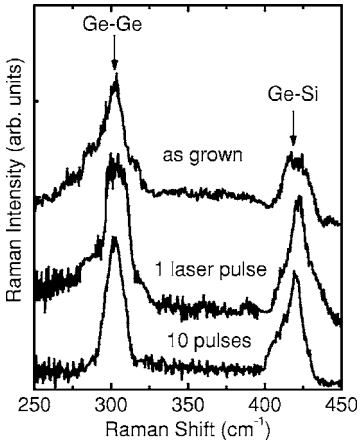

FIG. 2. Raman spectra of Ge QD samples before and after pulsed laser annealing.

III. EXPERIMENTAL RESULTS

A. Raman spectroscopy

The samples were first characterized by Raman spectroscopy to estimate the structural changes in Ge nanoclusters induced by a ruby laser irradiation. Figure 2 shows the Raman spectra of the as-grown QD sample and of the samples modified by one and ten laser shots. A peak observed at ~305 cm^{-1} is originated from the optical vibration of Ge-Ge bonds in Ge islands. Another feature at ~420 cm^{-1} corresponds to the local Ge-Si vibrations.

Based on Raman measurements the Ge-Si intermixing effect can be found from the ratio of the integrated intensities of the Ge-Ge and Ge-Si peaks,[23]

$$\frac{I_{\text{Ge-Ge}}}{I_{\text{Si-Ge}}} = B\frac{x}{2(1-x)}, \tag{1}$$

where x is the Ge content in the nanoclusters and B is a constant which depends on the experimental conditions. We initially checked the validity of Eq. (1) for a number of thin SiGe layers with a known Ge content. In this way, we determined a coefficient B of 2.2 for our experimental conditions. Analysis shows that the laser processing results in a decrease of Ge content from ≳70% for the as-grown sample to ~50% for the sample subjected to 10 laser pulses.

A striking feature observed in Fig. 2 is the reduction of the width of the Ge-Ge band in the laser annealed samples. As the number of laser pulses increases to 10, the full width at half maximum of the Ge-Ge peak is reduced by a factor of ~1.5. Since the position of the Raman peak is determined by the optical phonon confinement effect and elastic strain distribution, this result implies that the nanosecond laser annealing can improve the homogeneity of the structural characteristics of Ge nanoclusters.

B. Space-charge spectroscopy

1. Capacitance-voltage characteristics

Figure 3 shows experimental capacitance-voltage (C-V) characteristics (symbols) for the reference and the dot

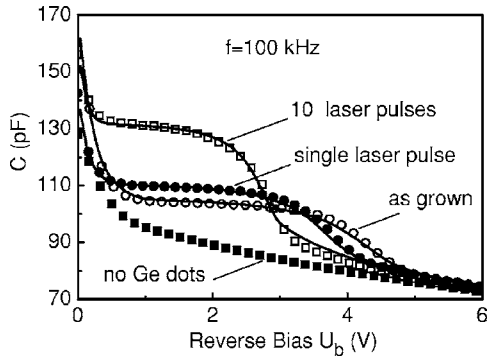

FIG. 3. Capacitance-voltage characteristics measured at modulation frequency of 100 kHz for the reference and dot samples before and after pulsed laser processing. Experimental data are shown by symbols and model simulations by solid lines.

samples before and after the pulsed laser irradiation. The traces were recorded at room temperature in order to ensure fast charge exchange between the QD's and the Si valence band at the modulation frequency of 100 kHz. At such low f, the C-V characteristics are frequency-independent, which is a manifestation of an equilibrium of the charging/discharging process.

The dependence of the capacitance on bias for the reference sample shows no specific features and has the form of the conventional C-V characteristic of a p-type Schottky diode. For the dot samples, we observe a plateaulike structure caused by an additional capacitance associated with the positive charge accumulation in the dot layer. Due to the p-type modulation doping in the Si matrix, the Ge QD's are charged by holes at a zero bias. When a reverse bias is applied to the diode, the holes are gradually swept out. At $U_B \gtrsim 4$ V for the as-grown sample, $U_B \gtrsim 3.5$ V and 2.5 V for the samples irradiated with 1 and 10 laser pulses, respectively, holes escape from QD's and the latter become neutral.

As a first approximation, the width of the capacitance plateau ΔU_B can be used to estimate the average number of holes accumulated in each dot by $N_h=(C/qSn_{\mathrm{QD}})\Delta U_B$, where $q>0$ is the elementary charge, C is the capacitance of the plateau, S is the contact area, and n_{QD} is the dot density. For $\Delta U_B \sim 4$ V, $C \sim 100$ pF, $n_{\mathrm{QD}}=4\times10^{11}$ cm^{-2}, we estimate $N_h \sim 2$. This means that, at $U_B=0$ V, the only ground state is filled with two holes; the highest energy states of the dots are empty and cannot be measured by space-charge spectroscopy.

For a numerical analysis, we used a quasistatic charging model proposed by Brounkov *et al.*[24] and developed later by Wetzler *et al.*[25] and Chang *et al.*[26] The charge distribution and the band bending profile were determined from the self-consistent solving the one-dimensional Poisson equation

$$\partial_z[\epsilon(z)\partial_z\phi(z)]\epsilon_0 = -\rho(z), \tag{2}$$

where ϕ is the electrostatic potential, ϵ and ϵ_0 are the relative and absolute permittivities, respectively, and ρ is the charge density. The total charge density in the bulk includes the density of free holes, p and ionized acceptors, N_A^-:

$$\rho(z) = q[p(z) - N_A^-(z)], \tag{3}$$

where

$$p(z) = N_v F_{1/2}\left(\frac{E_v(z) - E_{fp}(z)}{k_B T}\right), \tag{4}$$

$$N_A^-(z) = \frac{N_A(z)}{1 + 4\exp[(E_v(z) + E_A - E_{fp}(z))/k_B T]}, \tag{5}$$

$$E_v(z) = E_{v0} - \phi(z). \tag{6}$$

Here, N_v is the effective density of states in the valence band, $F_{1/2}$ is the Fermi function, E_v is the valence band edge, E_{fp} is the Fermi quasilevel for holes, N_A is the boron concentration, E_A is the boron ionization energy, and E_{v0} is the valence band edge at $z=w$ where w is the depletion width.

For simplicity, the holes confined in the dots are considered as the pointlike charges. QD's enter the problem through the boundary condition

$$\left.\frac{d\phi}{dz}\right|_{z=L+0} - \left.\frac{d\phi}{dz}\right|_{z=L-0} = \frac{qp_{\mathrm{QD}}}{\epsilon\epsilon_0}, \tag{7}$$

where L is the position of the QD layer from the surface, p_{QD} is the density of holes in the dots. The hole density trapped in the dots can be expressed as

$$p_{\mathrm{QD}} = \frac{n_{\mathrm{QD}}}{E_\sigma\sqrt{2\pi}}\int \exp\left[-\frac{1}{2}\left(\frac{E-E_1}{E_\sigma}\right)^2\right][f^{(1)} + 2f^{(2)}]dE, \tag{8}$$

where $f^{(1)}$ and $f^{(2)}$ are the probabilities of the dot to accumulate one or two holes, respectively, E_1 is the confinement energy of a hole in the ground state with respect to the Si valence band edge, E_σ is the standard energy deviation which corresponds to the spread of energy levels in array of the dots. Similar to the case of multicharged centers in semiconductors, the probabilities $f^{(1)}$ and $f^{(2)}$ can be calculated using the Grand Canonical Gibbs function. This is given by

$$f^{(1)} = \frac{g_1\exp\left(-\frac{E_{fp}-E_1}{k_B T}\right)}{g_0 + g_1\exp\left(-\frac{E_{fp}-E_1}{k_B T}\right) + g_2\exp\left(-\frac{2E_{fp}-(E_1+E_2)}{k_B T}\right)}$$

and

$$f^{(2)} = \frac{g_2\exp\left(-\frac{2E_{fp}-(E_1+E_2)}{k_B T}\right)}{g_0 + g_1\exp\left(-\frac{E_{fp}-E_1}{k_B T}\right) + g_2\exp\left(-\frac{2E_{fp}-(E_1+E_2)}{k_B T}\right)},$$

where E_2 is the energy of two holes in the ground state (E_1 and E_2 are separated by the Coulomb interaction), g_0, g_1, and g_2 are the degeneracies of the hole state when, respectively, emptied and filled with one or two holes. Here we used $g_1=2$ for a single occupied state and $g_2=1$ for the dots occupied with two holes. After determining the potential dis-

TABLE I. The energies of one (E_1) and two (E_2) holes in the ground state of the dots, the energy dispersion E_σ, and the QD density n_{QD} obtained from numerical analysis of the capacitance-voltage characteristics. The accuracy of the $E_{1,2}$ data is ±20 meV, E_σ was determined with the error of ±10 meV, and the accuracy values of n_{QD} is 5×10^{10} cm^{-2}.

Sample	E_1 (meV)	E_2 (meV)	E_σ (meV)	n_{QD} (cm^{-2})
as-prepared	320	270	110	4.5×10^{11}
irradiated of 1 laser pulse	350	280	90	3.6×10^{11}
irradiated of 10 laser pulses	360	320	60	3.3×10^{11}

tribution at different biases U_B, the differential capacitance was then calculated as $C(U_B)=\Delta Q_s/\Delta U_B$, where $Q_s=-\epsilon\epsilon_0 S d\phi/dz|_{z=+0}$ is the total charge in the structure and $-d\phi/dz|_{z=+0}$ is the electric field near the semiconductor surface. The optimal simulated C-V curves are shown in Fig. 3 by solid lines. The fitting parameters are listed in Table I. The claimed accuracy ensures minimal mean-square deviation of the calculated data from the experimental one.

Usually, to obtain reliable values from simulation of C-V characteristics, the number of fitting parameters used are varied from two[24,25] to five.[26] Here we used four variable parameters, of which three are energy values E_1, E_2, and E_σ, and the fourth is the quantum dot density n_{QD}. We can check the validity of this procedure by making an analysis of the values of parameters which correspond to the best fit. First, recent calculations based on the sp^3 tight-binding approach[27] demonstrated that the ground state energy of the hole confined in a pyramid-shaped Ge QD with a lateral size of ~10 nm is ~330 meV, which is very close to the energies deduced from the C-V analysis. Second, in the framework of the simplified model, the intradot Coulomb charging energy is given by $E_C=e^2/C_{QD}$, where C_{QD} is the capacitance of the dots. Assuming the QD to be a disk with a capacitance $C_{QD}=4\epsilon_0\epsilon_{Ge}\ell$ and a diameter $\ell=10$ nm, we obtain $E_C=40$ meV which is in a reasonable agreement with the quantity $\Delta=E_1-E_2$. Third, the value of $E_\sigma\sim100$ meV extracting from fitting is quite close to the width of QD-related PL peak reported in Ref. 28 for Ge QD's with $\ell\approx10$ nm. Fourth, the QD density, $(4.5\pm0.5)\times10^{11}$, found from the simulation of the C-V characteristic for the as-prepared sample agrees well with that determined independently from STM measurements, $(4.0\pm0.5)\times10^{11}$ cm^{-3}. Thus we may conclude that fitting procedure works correctly.

Two important observations can be made in Table I. First, after the laser treatment, the hole level depth tends to increase. This is explained by the increase of the average QD size in ensemble due to laser-induced dissolving the small Ge islands and swelling out the large Ge dots because of the atomic intermixing at the Ge/Si interface. Diminishing of the effective dot density supports this assertion. Second, the spread of the hole energy levels is reduced in the laser-irradiated samples, which testifies for the substantial improvement of the uniformity of QD's sizes stimulated by nanosecond laser processing. In particular, after the treatment with 10 pulses the dispersion of hole energies is reduced by a factor of about 2.

2. Admittance spectroscopy

Admittance spectroscopy is a well-known method to characterize deep impurity levels in semiconductors.[29] In these measurements, the ac conductance G of the sample is measured as a function of temperature for a fixed reverse bias U_B and test frequency $\omega=2\pi f$. For a QD system the mechanism of ac response is suggested to be similar to those commonly considered for deep defect states. An analysis of the QD ac response based on the Shockley-Read-Hall dynamics was made by Chang *et al.*[30] The small ac voltage with a frequency ω will alternatively fill and empty the QD carrier levels. The thermionic emission rate of holes from the dots as well as from deep impurities depends exponentially on temperature[31] T, i.e., $e_p(T)=A\sigma T^2\exp(-E_{act}/k_BT)$, where A is a temperature independent factor, σ is the capture cross section, E_{act} is the activation energy being determined by the actual path whereby holes escape from the dots to the Si valence band. Following this approach, the QD ac conductance is given by[30]

$$G(\omega,T)=Sq^2n_{QD}N_q\frac{\partial\phi}{\partial U_B}\frac{f_e(1-f_e)}{k_BT}\left(\frac{\omega^2\tau}{1+\omega^2\tau^2}\right), \qquad (9)$$

where N_q is the number of quantum hole states in the dot, $\partial\phi/\partial U_B$ represents the change of the potential at the QD layer caused by the increment of the applied bias ∂U_B, f_e is the QD equilibrium occupation fraction, and $\tau=(1-f_e)/e_p$ is the characteristic time for the hole exchange between the QD's and the barrier. For a given measurement frequency, the conductance reaches a maximum at a temperature T_{max} which corresponds to the condition

$$e_p(T_{max})\approx\omega/2. \qquad (10)$$

Thus, by measuring the $G(T)$ dependencies at various ω, the activation energies of hole emission rate can be deduced from the Arrhenius plot of $e_p(T_{max})/T_{max}^2$ vs $1/T_{max}$.

Figure 4 shows the temperature dependencies of the conductance for different samples. The curves were measured at $U_B=2$ V and $f=150$ kHz. As in the case of C-V characteristics, the conductance spectrum of the sample without Ge QD's shows no specific features. For the Schottky diodes with QD's, the $G(T)$ traces exhibit maxima whose amplitude G_{max} is proportional to the number of holes being exchanged between the Ge dots and the Si valence band. In this case, the temperature-frequency and temperature-bias mapping for the QD conductance can serve as a probe of energy level distribution in the dots.

The contour plots of temperature-frequency and temperature-bias conductance mapping for the as-grown dot sample are displayed in Figs. 5(a) and 5(b), respectively. For each investigated bias voltage, conductance spectra have

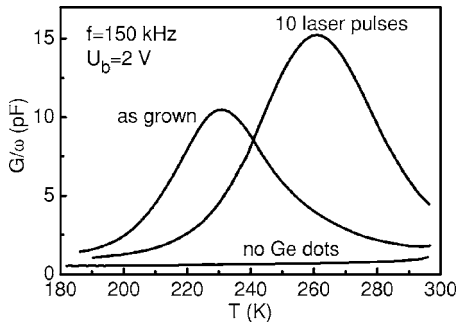

FIG. 4. Temperature dependencies of the conductance measured at a bias voltage of 2 V and modulation frequency of 100 kHz for the reference and dot samples before and after pulsed laser treatment.

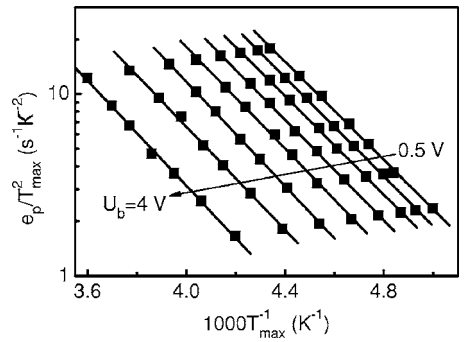

FIG. 6. The Arrhenius plots of the hole emission rate obtained from *G--T* spectra with different bias voltages for the as-grown sample.

been taken for 14 measurement frequencies. Similar measurements were also performed for the samples modified by one and ten laser pulses. The behavior of $G(T)$ can be qualitatively explained as follows. At a fixed bias, the charging/discharging process corresponds to the QD hole level coinciding with the Fermi level in the p^+-Si substrate. The rate of hole emission from this level becomes slower when the temperature is reduced; therefore, with a decrease in the modulation frequency, the condition for the maximum conductance (10) is satisfied at lower temperatures [Fig. 5(a)]. With an increase in reverse bias, the holes localized at deeper QD levels, for which condition (10) at a fixed frequency is satisfied at higher temperatures, contribute to the conductance. For this reason, the conductance peak in Fig. 5(b) shifts towards higher temperatures with increasing U_B. At $U_B > 4$ V, Ge QD's become completely depleted and the maximum on the $G(T)$ curve disappears. This is consistent with the observation from the C-V measurements of the same sample.

Figure 6 shows the typical dependencies $e_p/T^2_{\max}(T^{-1}_{\max})$ obtained from the temperature variation under different modulation frequencies for the as-grown sample. The activation energies E_{act} of the hole emission rate were found from the slope of the approximating straight lines. The linear correlation coefficients of all the lines are larger than 0.999. The resulting energies E_{act} before and after the nanosecond pulsed laser irradiation are shown in Fig. 7 as a function of reverse bias voltage. Their values are found to be quite close to the ground state hole levels $E_{1,2}$ deduced from the capacitance measurements but still about 30-50 meV smaller than $E_{1,2}$. This implies that the hole escape process in Ge/Si(001) QD's is a two-step process[26,30,32–34] which involves thermal activation to the excited state located within the range of 30-50 meV above the Si valence band edge in the QD's or in the wetting layer and then subsequent tunneling into the Si by the assistance of electric field.

For all samples, the activation energy decreases with decreasing of the bias voltage, and the range of energy variation ΔE, in the interval U_B where the capacitance plateau is observed, diminishes after the laser action. With increasing of the reverse bias, the chemical potential scans through the density of hole states in the QD layer. At higher reverse bias, the chemical potential crosses deeper states in the dots. In QD's, which can be charged by more than two carriers and in which conclusively higher energy levels than the ground state are occupied, the dependence of the activation energy on the QD occupation is usually attributed to the state-filling effect.[35,36] However the effect of state-filling is not relevant in a system of small QD's which are studied in this paper and

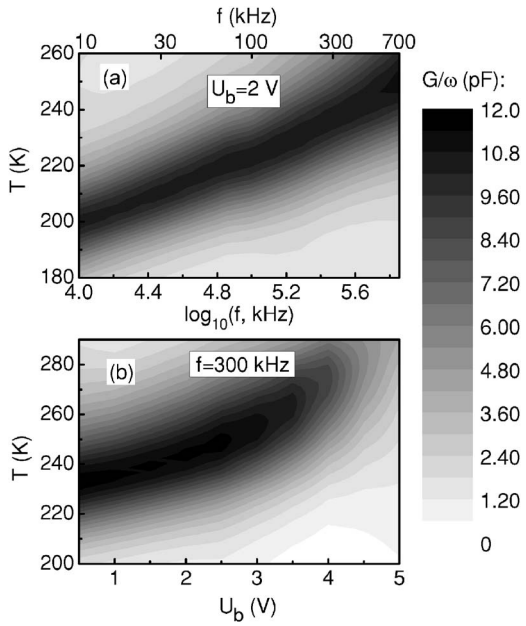

FIG. 5. Contour plots of (a) temperature-frequency and (b) temperature-bias conductance mapping for as-grown dot sample.

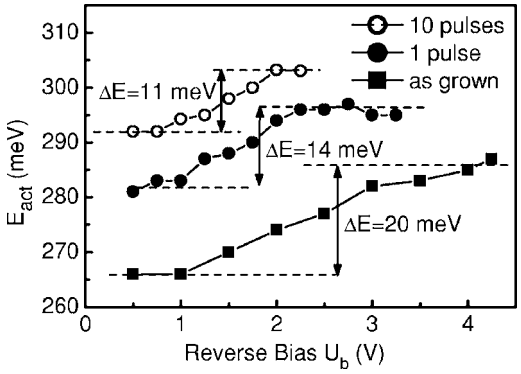

FIG. 7. Bias dependent activation energies of hole emission rate before and after pulsed laser processing.

contain no more than two holes. Thus, the change of the activation energy with bias may be attributed to the dispersion of the hole ground state eigenenergy due to the size distribution of the quantum dots. Following this interpretation, the parameter ΔE should reflect the spread of hole energy levels in array of the dots. Reducing ΔE after the laser treatment allows us again to conclude that the pulsed laser action does lead to the decrease of the hole energy dispersion.

The question is why the energy variation ΔE is about five times smaller than the standard energy deviation E_σ obtained from simulation of the capacitance data. The probable explanation is that, in fact, the parameter ΔE is rather related to variation of energy difference between the ground state and the excited state involved into the two-step hole escape process. When the size of Ge QD is changed, the energy levels of both ground and excited states move in the same direction relative to the Si valence band and, hence, the change of the energy gap between them with changing QD size is smaller than the displacement of each separate level. In particular, if the interlevel spacing in QD did not depend on the dot size ℓ than $\Delta E=0$.

We can check this explanation by using theoretical calculations of the hole energy spectrum as a function of ℓ for real pyramid-shaped Ge QD's in Si.[27] Recalculating the data for the dot lateral size $\ell \sim 10$ nm presented in Fig. 1 of Ref. 27 one can find the following incremental changes $\partial E_{\mathrm{gr}}/\partial \ell \approx 20$ meV/nm and $\partial(E_{\mathrm{gr}}-E_{\mathrm{ex}})/\partial \ell \approx -2$ meV/nm, where E_{gr} and E_{ex} are the energies of the ground and the first excited states, respectively. Clearly, these two derivatives differ from one another by one order providing support for the our explanation.

IV. SUMMARY

In summary, Raman and space-charge spectroscopies were used to study effect of nanosecond pulsed ruby laser processing on the composition and hole energy spectrum of Ge self-assembled quantum dots coherently embedded in a Si matrix. The inhomogeneity of quantum dot array parameters owing to Ge nanocluster size dispersion inherent in the Stranskii-Krastanov growth was found to be noticeably improved with subsequent laser irradiation from single up to ten pulses action.

ACKNOWLEDGMENTS

We thank A. V. Nenashev for assistance in development of a simulation procedure. The work was supported by INTAS (01-0615), RFBR (No. 03-02-16526), and the Integration Project between Siberian Branch of the Russian Academy of Sciences and the Belarus National Academy of Sciences (No. 186). A.I.Y. acknowledges financial support from the State program for support of young Russian doctors of sciences (No. MD-28.2003.02).

*Electronic address: yakimov@isp.nsc.ru

[1] D. Bimberg, M. Grundmann, and N. N. Ledentsov, *Quantum Dot Heterostructures* (Wiley, Chichester, 1998).

[2] A. I. Yakimov and A. V. Dvurechenskii, in *Intersubband Infrared Photodetectors, Selected Topics in Electronics and Systems Series*, edited by V. Ryzhii (World Scientific, Singapore, 2003), Vol. 27, p. 281.

[3] Y. Ono, A. Fujiwara, K. Nishiguchi, H. Inokawa, and Y. Takahashi, J. Appl. Phys. **97**, 031101 (2005).

[4] N. S. Beattie, B. E. Kardynał, A. J. Shields, I. Farrer, D. A. Ritchie, and M. Pepper, Phys. Rev. B **70**, 081304(R) (2004).

[5] D. Loss and D. P. DiVincenzo, Phys. Rev. A **57**, 120 (1998).

[6] A. I. Yakimov, A. V. Dvurechenskii, Yu. Yu. Proskuryakov, A. I. Nikiforov, O. P. Pchelyakov, S. A. Teys, and A. K. Gutakovskii, Appl. Phys. Lett. **75**, 1413 (1999).

[7] O. P. Pchelyakov, Ye. B. Bolkhovityanov, A. V. Dvurechenskii, L. V. Sokolov, A. I. Nikiforov, A. I. Yakimov, and B. Voigtländer, Semiconductors **34**, 1229 (2000).

[8] J. Drucker and S. Chaparro, Appl. Phys. Lett. **71**, 614 (1997).

[9] X. Wang, Z. Jiang, H. Zhu, F. Lu, D. Huang, X. Liu, C. Hu, Y. Chen, Z. Zhu, and T. Yao, Appl. Phys. Lett. **71**, 3543 (1997).

[10] T. P. Munt, D. E. Jesson, V. A. Shchukin, and D. Bimberg, Appl. Phys. Lett. **85**, 1784 (2004).

[11] J. Tersoff, C. Teichert, and M. G. Lagally, Phys. Rev. Lett. **76**, 1675 (1996).

[12] E. Mateeva, P. Sutter, J. C. Bean, and M. G. Lagally, Appl. Phys. Lett. **71**, 3233 (1997).

[13] V. L. Thanh, V. Yam, P. Boucaud, Y. Zheng, and D. Bouchier, Thin Solid Films **369**, 43 (2000).

[14] C. S. Peng, Q. Huang, W. Q. Cheng, J. M. Zhou, Y. H. Zhang, T. T. Sheng, and C. H. Tung, Phys. Rev. B **57**, 8805 (1998).

[15] A. Portavoce, F. Volpi, A. Ronda, P. Gas, and I. Berbezier, Thin Solid Films **380**, 164 (2000).

[16] J. Zhu, K. Brunner, and G. Abstreiter, Appl. Phys. Lett. **73**, 620 (1998).

[17] A. I. Nikiforov, V. A. Ulyanov, O. P. Pchelyakov, S. A. Tiis, and A. K. Gutakovskii, Phys. Solid State **47**, 67 (2005).

[18] A. V. Dvurechenskii, J. V. Smagina, V. A. Zinovyev, S. A. Teys, A. K. Gutakovskii, and R. Groetzschel, Int. J. Nanosci. **3**, 19 (2004).

[19] V. Yu. Balandin, A. V. Dvurechenskii, and L. N. Aleksandrov, Phys. Status Solidi A **110**, 133 (1988).

[20] V. A. Volodin, E. I. Gatskevich, A. V. Dvurechenskii, M. D. Efremov, G. D. Ivlev, A. I. Nikiforov, D. A. Orekhov, and A. I. Yakimov, Semiconductors **37**, 1315 (2003).

[21] G. D. Ivlev and E. I. Gatskevich, Appl. Surf. Sci. **143**, 265 (1999).

[22] A. V. Kolobov, J. Appl. Phys. **87**, 2926 (2000).

[23] P. M. Mooney, F. H. Dacol, J. C. Tsang, and J. O. Chu, Appl. Phys. Lett. **62**, 2069 (1993); J. C. Tsang, P. M. Mooney, F. Dacol, and J. O. Chu, J. Appl. Phys. **75**, 8098 (1994).

[24] P. N. Brounkov, S. G. Konnikov, V. M. Ustinov, A. E. Zhukov, A. Yu. Egorov, M. Maximov, N. N. Ledentsov, and P. S. Kop'ev, Semiconductors **30**, 492 (1996); P. N. Brounkov, A.

Polimeni, S. T. Stoddart, M. Henini, L. Eaves, P. C. Main, A. R. Kovsh, Yu. G. Musikhin, and S. G. Konnikov, Appl. Phys. Lett. **73**, 1092 (1998).

[25] R. Wetzler, A. Wacker, E. Schöll, C. M. A. Kapteyn, R. Heitz, and D. Bimberg, Appl. Phys. Lett. **77**, 1671 (2000).

[26] W.-H. Chang, W. Y. Chen, T. M. Hsu, N.-T. Yeh, and J.-I. Chyi, Phys. Rev. B **66**, 195337 (2002).

[27] A. V. Dvurechenskii, A. V. Nenashev, and A. I. Yakimov, Nanotechnology **13**, 75 (2002).

[28] A. I. Yakimov, A. V. Dvurechenskii, V. V. Kirienko, N. P. Stepina, A. I. Nikiforov, V. V. Ul'yanov, S. V. Chaikovskii, V. A. Volodin, M. D. Efremov, M. K. Seksenbaev, T. S. Shamirzaev, and K. S. Zhuravlev, Semiconductors **38**, 1225 (2004).

[29] See, for example, D. L. Losee, Appl. Phys. Lett. **21**, 54 (1972); G. Vincent, D. Bois, and P. Pinard, J. Appl. Phys. **46**, 5173 (1975).

[30] W.-H. Chang, W. Y. Chen, M. C. Cheng, C. Y. Lai, T. M. Hsu, N.-T. Yeh, and J.-I. Chyi, Phys. Rev. B **64**, 125315 (2001).

[31] D. V. Lang, J. Appl. Phys. **45**, 3023 (1974).

[32] C. M. A. Kapteyn, F. Heinrichsdorff, O. Stier, R. Heitz, M. Grundmann, N. D. Zakharov, D. Bimberg, and P. Werner, Phys. Rev. B **60**, 14265 (1999).

[33] C. M. A. Kapteyn, M. Lion, R. Heitz, D. Bimberg, P. N. Brunkov, B. V. Volovik, S. G. Konnikov, A. R. Kovsh, and V. M. Ustinov, Appl. Phys. Lett. **76**, 1573 (2000).

[34] K. Schmalz, I. N. Yassievich, P. Schittenhelm, and G. Abstreiter, Phys. Rev. B **60**, 1792 (1999).

[35] C. M. A. Kapteyn, M. Lion, R. Heitz, D. Bimberg, C. Miesner, T. Asperger, K. Brunner, and G. Absreiter, Appl. Phys. Lett. **77**, 4169 (2000).

[36] M. Geller, C. Kapteyn, L. Müller-Kirsch, R. Heitz, and D. Bimberg, Appl. Phys. Lett. **82**, 2706 (2003).